V.YO. STADNYK, P.A. SHCHEPANSKYI, M.YA. RUDYSH, R.B. MATVIIV,
R.S. BREZVIN

Ivan Franko National University of Lviv
(19, Drahomanova Str., Lviv 79023, Ukraine; e-mail: vasylstadnyk@ukr.net)

CONCENTRATION DEPENDENCES OF DIELECTRIC PARAMETERS OF IMPURITY-DOPED K_2SO_4 CRYSTALS

The influence of a copper impurity with various concentrations on the unit cell parameters, band-energy structure, and refractive characteristics of potassium sulfate crystals has been studied. The unit-cell parameters and volume of impurity-doped crystals are found to increase almost linearly with the growth of the impurity content. At the same time, the refractive indices n_i $(i = x, y, z)$ of doped crystals slightly decrease (by about 2.5×10^{-3}), but the relations $n_z >$ $> n_x > n_y$ and $dn_z/d\lambda > dn_x/d\lambda > dn_y/d\lambda$ between them remain unchanged. The energy band structure of crystals with a copper content of 1.7% is calculated. It is found that the forbidden gap decreases, as the impurity concentration increases. Five localized levels corresponding to d-electron states of Cu^{2+} impurity ions are identified in the band gap. It is established that the top of the valence band is formed by the oxygen p-states, and the bottom of the conduction band by the 3s- and 4s-states of the sulfur and potassium atoms. The localized 4s-states of copper atoms are located at the bottom of the conduction band. The concentration dependences of the density and ionic radius are analyzed.

K e y w o r d s: crystal, impurity, refractive index, birefringence, unit cell, energy band structure, forbidden gap.

1. Introduction

Potassium sulfate (K_2SO_4) crystals (PSCs) are typical representatives of the crystals belonging to the $ABSO_4$-group. The PSCs are ferroelectric insulators, which are transparent in the visible spectral interval and demonstrate a phase transition. Two their phase modifications are known: β-K_2SO_4 at temperatures below 587 °C and α-K_2SO_4 at higher temperatures. The crystal lattice of the α-K_2SO_4 crystal can be described by a hexagonal basis with the following crystal lattice parameters: $a = 5.90(2)$ Å and $c = 8.11(3)$ Å [1–4]. The corresponding spatial symmetry group is $P6_3/mmc$. In the low-temperature

β-K_2SO_4 phase (below 860 K), the unit cell contains four formula units and has the parameters $a = 0.05731$ nm, $b = 1.008$ nm, and $c = 0.7424$ nm. The c-axis is pseudohexagonal. The atomic group SO_4^{2-} in PSCs forms a rigid tetrahedron with the sulfur ion arranging at its center and the oxygen ions at its vertices [5–7].

The PSCs are widely used in optoelectronics and crystal optics (as sensors of temperature, pressure, and electromagnetic radiation), as well as for acousto-optical modulation of ultraviolet radiation. However, the scope of their application permanently extends, and the operating conditions become more complicated. The corresponding arising problems demand that the behavior of structural materials under extreme conditions should be predicted, the available

physical properties should be modified, or new materials with specific characteristics should be created [8].

The most vivid example of changing the physical properties is the creation of defects in the crystal lattice as a result of radiation-chemical processes. The knowledge of the mechanisms of their creation and transformation makes it possible to perform a purposeful search for radiation-resistant and radiation-sensitive materials that could be used as structural materials in various domains of technology.

One of the simplest methods to vary the optical and dielectric properties of crystals is the application of external factors or doping the crystals with various substitutional impurities. Transition-metal ions are well suited for this task because they are one of the traditional activators for studying the spectral and radiation properties of crystals.

Earlier, the influence of impurities on the dielectric parameters of PSCs was studied in works [9–14]. It was found that the dielectric constant and the dielectric loss coefficient for PSCs crystals with the impurities of Cu^{2+} and Fe^{2+} ions [9, 10] gradually decrease as the frequency increases. This behavior was explained by the influence of polarized Fe^{2+} ions on the octahedral environment of the crystal structure.

In the case of the Co^{2+} impurity introduction, three new absorption bands with maxima at 4.57, 4.96, and 5.85 eV, which are associated with activator absorption, are observed at room temperature in the energy interval of 4.0–6.2 eV [11]. The optical density of absorption bands increases with the growing concentration of impurity centers [12]. The cited authors associated the increase in the number of absorption bands at lower temperatures with the reduction of the optical band width, which leads to band splits that are unobservable at higher temperatures.

The corresponding changes were detected in works [13–15] after the introduction of Ni^{2+} and Mn^{2+} impurities: there appeared new absorption bands at room temperature. Irrespective of the manganese sulfate concentration in the initial solution – and, accordingly, the impurity concentration in the crystal – the optical density in the impurity absorption bands depends linearly on the specimen thickness. The impurity absorption centers are uniformly distributed over the specimen volume. If the content of impurity salt in the initial solution is higher (accordingly, the

impurity concentration in the crystal is also higher), the linearity becomes violated.

The influence of copper impurity with various concentrations on the optical parameters (the refractive indices and the birefringence) of PSCs was analyzed in works [16–19]. It was found that the introduction of impurities leads to the reduction of the absolute values of refractive indices but does not affect the character of their dispersion. It also modifies the absolute values of birefringence and leads to a stronger temperature dependence $\Delta n_i(T)$ in comparison with the pure crystal.

At room temperature, the PSC is optically biaxial. However, as the temperature changes in the interval of 300–850 K, it twice undergoes transitions into an optically uniaxial state (which corresponds to the appearance of isotropic points) not associated with structural transformations. It was revealed that the introduction of impurities shifts the isotropic points towards lower temperatures in comparison with the pure crystal [19]. The structure of PSCs with a copper impurity concentration of 3% was studied by means of X-ray powder diffraction. It was found that this structure can be considered as a result of multiple (two potassium atoms per copper atom) heterovalent substitution of two K^+ ions in the structure by the Cu^{2+} ion [17].

However, there is a lack of information in the literature concerning clear dependences of the dielectric parameters of PSCs on the concentration of introduced impurities. The aim of this work was to analyze the dependence of the unit cell parameters, the band gap width, and the crystal optical characteristics of PSCs on the concentration of introduced copper impurities in order to enable the production of crystals with predetermined properties.

2. Results and Their Discussion

2.1. Unit cell parameters and band-energy structure of impurity-doped crystals

The crystal structure of PSCs doped with copper (to a concentration of 1.7% or 3%) was studied using the X-ray powder diffraction (XRPD) method. The analysis of the results obtained showed that for the indicated impurity concentrations, the spatial symmetry group does not change and equals $Pnma$, $Z = 4$. For PSCs with a copper impurity concentration of 1.7%, the
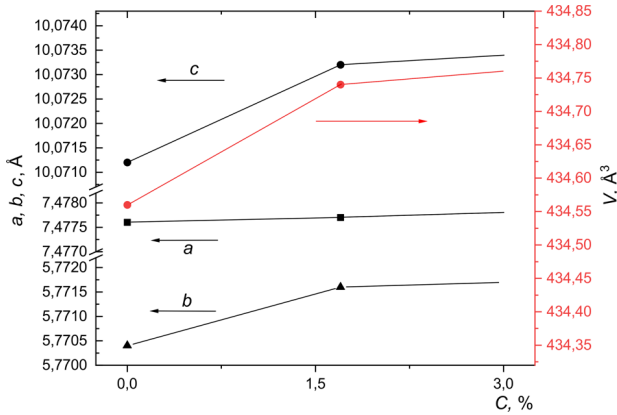
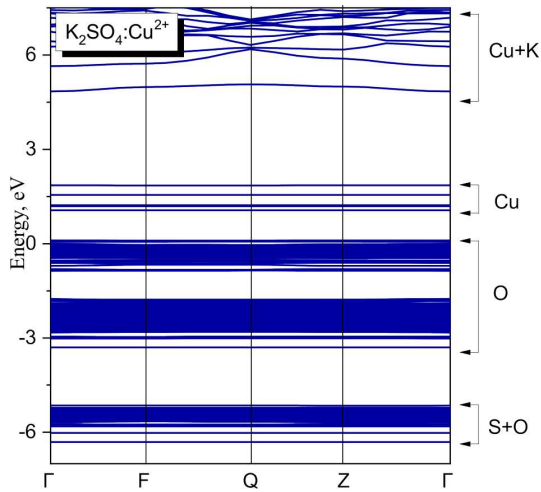**Fig. 1.** Concentration dependences of the unit cell parameters for impurity-doped K_2SO_4 crystals

Fig. 2. Energy band structure of K_2SO_4 crystals with a copper admixture content of 1.7% calculated using the GGA-PBE method

obtained unit cell parameters are $a = 7.4777(4)$ Å, $b = 5.7716(3)$ Å, $c = 10.0732(5)$ Å, and the unit cell volume is $V = 434.74(7)$ Å^3. For PS specimens with a copper impurity concentration of 3.0%, the corresponding parameters are $a = 7.4778(4)$ Å, $b = 5.7717(3)$ Å, $c = 10.0734(6)$ Å, and $V = 434.76(7)$ Å^3 [16].

In Fig. 1, the concentration dependences of the unit cell parameters and volume are shown for doped PSCs. One can see that they increase almost linearly with the increasing impurity concentration. However, the general metric of the crystal structure remains undeformed. These dependences, as well as the coor-

dinates of corresponding atoms, were used to calculate, by means of the DFT-GGA-PBE method [20–23] the electronic band structure $E(k)$ of the PSC with the 3%-admixture of copper ions Cu^{2+} and plot it at special points and along the high-symmetry lines in the Brillouin zone (BZ). The resulting band structure turned out very similar to that reported for the pure crystal [24, 25] and for isomorphic crystals [26, 27].

In order to assess the influence of the copper impurity concentration on the energy band structure, we additionally calculated the band structure for the PSC with the 1.7% copper content. In general, the electronic states are usually flat (have low dispersion) for PSCs with various impurity contents. The dispersion of the levels in the conduction band is higher, which points to a lower effective mass of charge carriers and their higher mobility. The valence band was found to consist of some narrow subbands separated by forbidden gaps (see Fig. 2). These subbands can provide additional electron transitions between them. Such transitions may be of interest from the core-valence luminescence aspect. An energy value of 0 eV corresponds to the valence band maximum. The forbidden gap is formed between the valence band top and the conduction band bottom, the both being located at the BZ center. The band gap widths are $E_g = 5.0$ and 4.92 eV for concentrations of 1.7% and 3.0%, respectively. Several electronic levels are localized in the forbidden gap. They correspond to the impurity electronic states of Cu^{2+} ions. A detailed analysis of the energy band structure allowed us to reveal a narrow set of five energy levels that correspond to d-electrons of copper and are located within the energy interval of 1.09–1.9 eV and 1.06–1.8 eV for copper impurity concentrations of 1.7% and 3.0%, respectively.

Figure 3 demonstrates the partial density of states constructed from individual contributions of one of the atoms, which makes it possible to identify the arrangement of electronic levels. One can see that the valence band top coincides with an energy of 0 eV formed by the oxygen p-states represented by the electronic levels within the interval from 0 to -5 eV. The electronic levels with lower energies in the interval from -6 to -8 eV are formed by the $2p$-, $3p$-, and $2s$-, $3s$-states of the oxygen and sulfur atoms. The observed sharp peak at -12 eV corresponds to the $3p$-states of the potassium atom. Two peaks at -18.4 and -22.3 eV are formed by the oxygen $2s$-states

hybridized with the sulfur 3p- and 3s-states, respectively. At -27.6 eV, a band formed by the 3s-states of the potassium atom is observed. The bottom of the conduction band is formed by the 3s- and 4s-electrons of the sulfur and potassium atoms. The localized 4s-states of the copper atom are arranged at the bottom of the conduction band. The splitting of the 3d-levels of the copper atom also takes place at energies of 1.09–1.9 eV.

Irrespective of the impurity concentration, the d-levels of electrons in the tetrahedral environment are split into two energy levels, e and t_2. The level e is double degenerate, while the t_2 one is triple degenerate and lies by about 10 Dq above the energy level e. Thus, the observed splitting of electronic d-states into more than two sublevels occurs due to the degeneracy elimination by the low-symmetry ligand field.

In Fig. 4, the concentration dependence of the forbidden gap width E_g of the PSC is shown. One can see that this quantity decreases almost linearly with the increasing concentration. This result correlates well with previously obtained ones for the baric dependence of E_g [24]. The cited authors showed that E_g increases at small compressions σ (the $dE_q/d\sigma$ magnitude has an order of 1 eV/GPa), which corresponds to the growth of the crystal density ρ. If we assume that the introduction of impurity leads to internal stresses, i.e., to crystal stretching, the forbidden gap width will decrease.

2.2. Concentration dependences of refractive indices and birefringence

The study of the refractive index dispersion $n_i(\lambda)$ of PSCs doped to Cu^{2+} ionic concentrations of 1.7% and 3.0% showed that it is normal in the spectral interval of 300–700 nm and drastically increases if approaching the absorption edge [17, 19]. The introduction of the admixture of Cu^{2+} ions leads to a reduction of the refractive indices n_i for the three crystallographic directions in the crystal with a maximum change of about 2.5×10^{-2} (Fig. 5). The relations $n_z > n_x > n_y$ for the refractive indices of pure crystals and $dn_z/d\lambda > dn_x/d\lambda > dn_y/d\lambda$ for their dispersion remain valid for the impurity-doped crystals. The largest decrease of the refractive index is observed for the direction X perpendicular to the plane of optical axes. Accordingly, for the impurity-doped crystals, a reduction of the magnitude and anisotropy
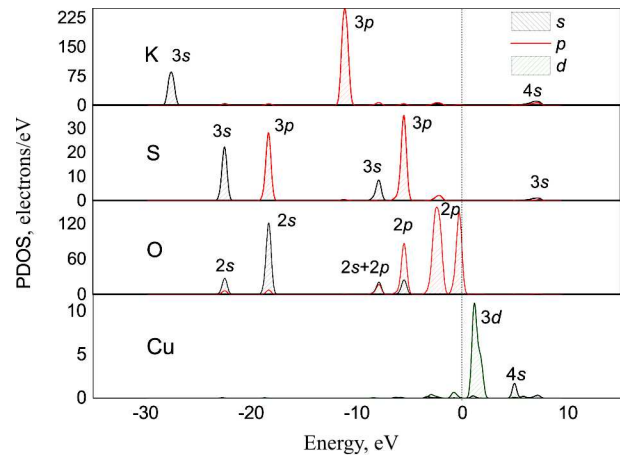
Fig. 3. Partial density of states of K$_2$SO$_4$: Cu^{2+}(1.7%) calculated using the GGA functional
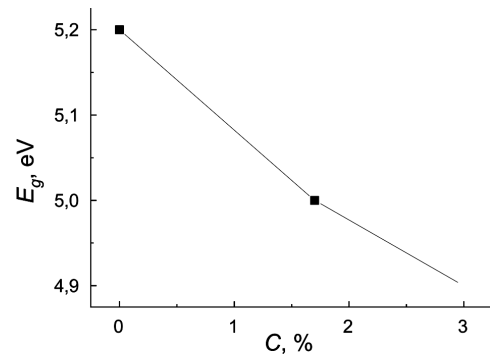
Fig. 4. Dependence of the band gap width on the copper impurity concentration in K$_2$SO$_4$ crystals
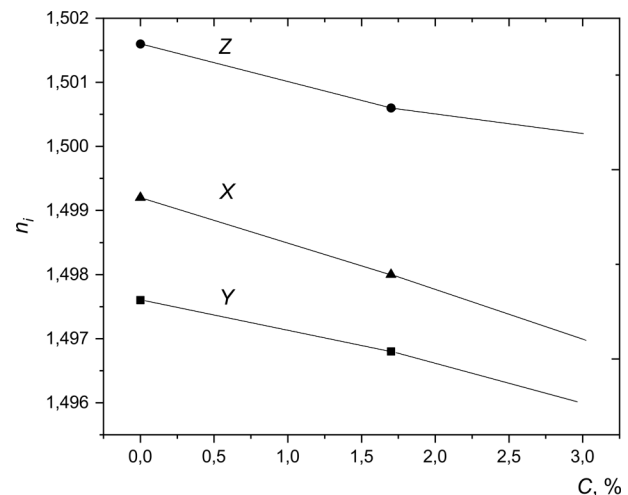
Fig. 5. Impurity-concentration dependences of the refractive indices in impurity-doped K$_2$SO$_4$ crystals
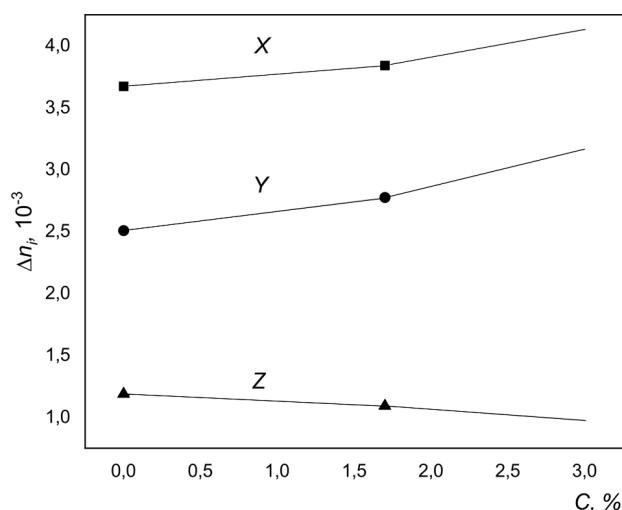
Fig. 6. Impurity-concentration dependences of the birefringence in impurity-doped K_2SO_4 crystals

of the optical indicatrix, as well as a slight decrease of the crystal anisotropy, takes place.

The birefringent properties of PSCs were studied with the help of the Obreimov spectral method. The refractive index values obtained using the Obreimov immersion method served as reference points. All birefringence studies were performed at room temperature and in the wavelength interval of 300–700 nm [28, 29]. It was found that the introduction of the impurity weakly changes the value of $\Delta n_i(\lambda)$ and does not affect the dispersion character $\left|\frac{\partial \Delta n_x}{\partial \lambda}\right| > \left|\frac{\partial \Delta n_y}{\partial \lambda}\right| > \left|\frac{\partial \Delta n_z}{\partial \lambda}\right|$. The following variations $\Delta n_i(\lambda)$ in the birefringence absolute values at a wavelength of 500 nm were revealed: in the X- and Y-directions, it increased by approximately 5.2×10^{-4} and 6.8×10^{-4} for impurity concentrations of 1.7% and 3.0%, respectively, and decreased by 1.4×10^{-4} and 2.1×10^{-4}, respectively, in the Z-direction (see Fig. 6). Furthermore, the value of $\frac{\partial \Delta n_x}{\partial \lambda}$ decreased from 3.5×10^{-6} nm^{-1} for the pure PSC to 3.2×10^{-6} nm^{-1} for the PSC with an impurity content of 1.7% and to 3.0×10^{-6} nm^{-1} for the PSC with an impurity content of 3.0%. The most substantial variation of the dispersion, $\Delta n_i(\lambda)$, was observed in the long-wavelength spectral section.

The observed changes in the birefringence of impurity-doped PSCs associated with the introduction of Cu^{2+} ions can considerably change the temperature and spectral positions of two isotropic points in the PSCs, which are observed at 617 and 700 K in the

pure PSC (for a wavelength of 500 nm). In our opinion, the origin of why the values of crystal-optical parameters change in impurity-doped crystals is as follows.

An inherent feature of PSCs is the ionic-covalent bond. Covalent bond manifests itself in the tetrahedral anionic groups, whereas the ionic bond is formed by the potassium ions located at the tetrahedron vertices. The K^+ ions are located in PSCs in two nonequivalent positions K1 and K2, the coordination environment of which is different. Cations K1 and K2 have a coordination environment of 10 and 9, respectively, relatively to the oxygen atom. The bases of SO_4 tetrahedra are in the K1O3 layer, and its vertices in the K2O layer. Since the K2O layers are almost plane, being shifted in the XY plane relatively to one another, the ions in one of the layers are located opposite the voids in the next K2O layer within the unit cell. The K1O3 layer is sandwiched between the K2O layers with zigzag gaps. As a result and due to the fact that the K1O3 plane and the K2O ones do not match in size, if those layers are overlapped, the K1O3 layer becomes deformed and corrugated. Hence, the dimensions of the orthorhombic unit cell and, accordingly, the optical parameters are governed by the ion packing in the K1O3 layers with and without corrugation, as well as by the mutual packing of the K1O3 and K2O layers.

Furthermore, the crystal structure of the copper-doped K_2SO_4 compound can be considered as the result of multiple (two potassium atoms per copper atom) heterovalent substitution of two K^+ ions by a Cu^{2+} one in the structure of the K_2CuSO_4 compound [17] or as the stacking of columns of SO_4^{2-} tetrahedra along the [0Y0] direction. The K atoms form zigzag chains in the space between those columns, and the copper atoms are located in the chains of the metal component. The K1 atoms are located in paired tetrahedral voids, and the copper atoms (the Cu^{2+} ion is paramagnetic by its nature [15]) at the boundary between the tetra- and octahedral voids in the second coordination environment. Bivalent copper ions randomly substitute cations. They mostly occupy positions that were previously occupied by K1 ions but slightly shifted to the base of one of the anion tetrahedra. Since the ordinal number of potassium is 19 and its atomic mass is 39 amu (for copper, these are 29 and 63.5 amu, respectively), such an increase of parameters occurs due to the atomic mass growth and

the change of ionic radius. The ionic radius decreases for metals if moving from left to right across the period. Therefore, more protons are added and metals lose their outer electron orbitals. But the outer valence shell remains unchanged so that the positively charged nucleus attracts electrons more strongly.

Using our results and the previously published ones on optoelectronic parameters, the correlation analysis of the latter was performed in order to establish a relationship between the values of refractive indices, birefringence, and forbidden gap width in impurity-doped PSCs. It was found that the refractive index decreases monotonically with the increasing crystal density (Table). In our opinion, this occurs owing to the polarization action of cations. In particular, as a result of the polarizing action of copper ions on the potassium electronic shells, the electron concentration in the interatomic space and the refractive index decrease.

The observed variations in the refractive indices of crystals are governed by lots of factors. In particular, these are the changes of the substance molecular weight and density, or the changes of the interatomic distances and hence the chemical bond strength. As the crystal density increases, the average value of the refractive index mainly increases. The density decrease can be associated with the reduction of the ionic radii of cations. For instance, if the cation radius decreases, the refractive index of the crystal diminishes almost linearly.

The analysis of the relation between the crystal structure and the refractive parameters can also be made on the basis of the following considerations. It is known [30–33] that the density ρ of many minerals containing the oxygen anion and their average atomic mass M (this is the molecular mass of the substance divided by the number of atoms in its chemical formula) is linearly related to their average refractive index n. This relationship means that the density is responsible for the refractive index value irrespective of the composition, phase, and crystal symmetry. This fact testifies that the refractive index of crystals increases with the growth of covalent component in the bond. A number of dependences have been proposed in the literature to describe the relationship between the refractive index and the density. The most famous are the Gladstone-Dale, Lorenz, Drude, and Allen laws. Their applicability to interpreting data on the density dependence of the refractive index was dis-

cussed in work [30]. In works [32, 33], it was shown that the formula for the refractive index dispersion can be used to derive relations that can be considered as the Gladstone-Dale and Drude laws. In work [33], it was found that experimental data for the refractive index n of most of simple inorganic compounds, except for alkali metal halides, can be represented by the following dependences:

$$n - 1 \propto C_1 \rho M^{-u_1}, \tag{1}$$

$$n^2 - 1 \propto C_2 \rho M^{-u_2}, \tag{2}$$

$$\frac{n^2 - 1}{n^2 + 2} \propto C_3 \rho M^{-u_3}, \tag{3}$$

where C_i are constants, and the values of the power exponents u_i are close to 0.4. Experimental data for alkali metal halides can also be described by the above equations.

For $ABSO_4$ crystals, it was found earlier [34] that their parameters u_i are larger, which points to a stronger power-law dependence between the density and the refractive index. Again, as for alkali metal halides [35], the coefficients C_i also differ from the mean statistical values and acquire much larger magnitudes. The closest to PSCs by the parameters C_i are alkali metal bromides ($C_1 = 0.991$ and $C_3 = 0.547$).

The refractive index can also change owing to the modification of coordination number, and this effect is stronger for the larger variation in the atomic coordination. The refractive indices of crystals increase together with the coordination numbers, the valence of the anions surrounding the cation at the same coordination numbers, and the concentration of binding electrons. This also occurs due to the expected reciprocal dependence of the refractive indices on the unit cell volume of any material.

The refractive indices can change not only owing to variations in the molar volume or the character of the chemical bond between atoms but also owing to the possible influence of chemical composition. The

Impurity-concentration dependences of the density and the ionic radius of impurity-doped K_2SO_4

C, %	r_{ion}, Å	ρ, g/cm^3
0.0	8.240	2.660
1.7	8.212	2.649
3.0	8.183	2.641

most practically important factor is the influence of crystallization water on the refractive index. It is well known that almost all crystals of the sulfate group are grown from the aqueous solution and therefore they contain crystallization water, which modifies the unit cell volume. Therefore, dehydration of the substance (i.e., the removal of the lightest and least refractive part from the substance formula unit) brings about the growth of the density and the refractive index.

3. Conclusions

To summarize, the influence of the copper impurity concentration on the unit cell parameters, the energy band structure, and the refractive parameters of potassium sulfate crystals is studied. It is found that the indicated parameters and the unit cell volume of impurity-doped crystals increase almost linearly with the impurity concentration growth. However, the general metric of the crystal structure remains undeformed. The spectral studies of the refractive parameters of synthesized crystals showed that the refractive indices n_i of impurity-doped crystals slightly decrease with a maximum change of 2.5×10^{-3}, but the relations $n_z > n_x > n_y$ and $dn_x/d\lambda > dn_x/d\lambda > dn_y/d\lambda$ between them remain unchanged.

The energy band structure of the crystal with the 1.7% copper content is calculated. A comparison with the pure crystal and the crystal with the 3% copper impurity content showed that the band gap decreases as the copper concentration grows: $E_g = 5.2, 5.0$, and 4.9 eV for concentrations of 0%, 1.7%, and 3.0%, respectively.

It is found that the introduction of impurities leads to the emergence of five localized levels in the forbidden gap, which correspond to the d-electron states of impurity Cu^{2+} ions. The levels are located within the energy intervals of 1.09–1.9 eV and 1.06–1.8 eV for the copper concentrations of 1.7% and 3.0%, respectively. In the tetrahedral environment, the electron d-levels are split into two energy levels, e and t_2. The level e is double degenerate, and the level t_2 is triple degenerate and, by energy, is arranged above the level e. The variation of the impurity concentrations within the examined interval of 1.7–3.0% does not affect the positions of those levels.

The partial density of electronic states was calculated. It was found that the top of the valence band is formed by the p-states of the oxygen atoms, and the bottom of the conduction band by the 3s- and 4s-states of the sulfur and potassium atoms. The localized 4s-states of copper atom are arranged at the bottom of the conduction band.

The correlation analysis of the refractive, structural, and electronic parameters of the crystals belonging to the K_2SO_4 group was performed. The refractive index of PSCs was found to grow with their average ionic radius, which is explained by the increase in the polarization action of cations. It was also revealed that the concentration growth of the introduced impurity leads to the reduction of the band gap width.

1. A.J. Van den Berg, F. Tuinstra. The space group and structure of α-K_2SO_4. *Acta Crystallogr. B* **34**, 3177 (1978).
2. S. Shiozaki, A. Sawada, Y. Ishibashi, Y. Takagi. Hexagonal-orthorhombic phase transition and ferroelasticity in K_2SO_4 and K_2SeO_4. *J. Phys. Soc. Jpn.* **43**, 1314 (1977).
3. H. Arnold, W. Kurtz, A. Richter-Zinnius, J. Bethke, G. Heger. The phase transition of K_2SO_4 at about 850 K. *Acta Crystallogr. B* **37**, 1643 (1981).
4. T.M. Chen, R.H. Chen. High-temperature structural phase transition of K_2SO_4 and K_2SeO_4 crystals studied by X-ray diffraction. *J. Solid State Chem.* **111**, 338 (1994).
5. K.S. Aleksandrov, B.V. Beznosikov. *Structural Phase Transitions in Crystals (Potassium Sulfate Family)* (Nauka, 1993) (in Russian).
6. B.V. Beznosikov, K.S. Aleksandrov. Crystal chemical regularities of changes in structures related to the α-K_2SO_4 type. Preprint No. 304 (Acad. Sci. USSR, 1985) (in Russian).
7. B.V. Beznosikov, K.S. Aleksandrov. Regularities in the formation of $ABCX_4$ structures. Preprint No. 463 (Acad. Sci. USSR, 1987) (in Russian).
8. L.I. Anatychuk. *Thermoelements and Thermoelectric Devices* (Naukova Dumka, 1979) (in Russian).
9. A.S. Baltabekov, T.A. Koketaitegi, L.M. Kim. Recombination processes in K_2SO_4 doped by ions of transitive metals. *Educat. Sci. Bord.* **2**, 131 (2011).
10. N. Mahadeva, A.S. Etalo. Electrical conductivity and phase transformation studies on pure and doped (Mg^{2+}, Zn^{2+}, Cu^{2+}, and Mn^{2+}) crystals of K_2SO_4. *Can. J. Chem.* **53**, 1542 (1975),
11. S. Radhakrishna, E.D. Pande. Transport properties of cobalt-doped potassium sulphate. *Phys. Status Solidi A* **16**, 433 (1973).

290

12. B.V.R. Chowdari, P. Venkateswarlu. Electron paramagnetic resonance of $Mn^{2\pm}$ in K_2SO_4 single crystal. *J. Chem. Phys.* **48**, 318 (1968).

13. A.S. Baltabekov, T.A. Koketajtegi, L.M. Kim, B.S. Tagayeva. Radiolisis of crystalohydrates alkaline metals. *Nauka i Studia. Physica* **2**, 91 (2011).

14. S.B. Anooza, R. Bertramb, D. Klimb. The solid state phase transformation of potassium sulfate. *Solid State Commun.* **141**, 497 (2007).

15. R.Yu. Abdusabirov, Yu.S. Gryaznov, M.M. Zapirov. Electron paramagnetic resonance of Cu^{2+} ions in K_2SO_4. *Phys. Solid State* **12**, 657 (1970).

16. V.Yo. Stadnyk, R.B. Matviiv, P.A. Shchepanskyi, M.Ya. Rudysh, Z.A. Kogut. Photoelastic properties of potassium sulfate crystals. *Phys. Solid State* **61**, 2130 (2019).

17. R.B. Matviiv, M.Ya. Rudysh, V.Yo. Stadnyk, A.O. Fedorchuk, P.A. Shchepanskyi, R.S. Brezvin, O.Y. Khyzhun. Structure, refractive and electronic properties of $K_2SO_4 : Cu^{2+}$ (3%) crystals. *Curr. Appl. Phys.* **21**, 80 (2021).

18. V.Y. Stadnyk, R.B. Matviiv, M.Y. Rudysh, R.S. Brezvin, P.A. Shchepanskyi, B.V. Andrievskii. Refractive parameters and band energy structure of K_2SO_4 crystals doped with copper. *J. Appl. Spectrosc.* **87**, 143 (2020).

19. V.Yo. Stadnyk, R.B. Matviiv, P.A. Shchepanskyi. Refractive and photoelastic properties of K_2SO_4 crystals doped with copper. *Crystallogr. Rep.* **65**, 961 (2020).

20. J.P. Perdew, J.A. Chevary, S.H. Vosko, K. Jackson, M.R. Pederson, D.J. Singh, C. Fiolhais. Atoms, molecules, solids, and surfaces: Applications of the generalized gradient approximation for exchange and correlation. *Phys. Rev. B* **46**, 6671 (1992).

21. *STOE & Cie GmbH, WinXPOW 3.03. Powder Diffraction Software Package* (Darmstadt, 2010).

22. W. Kraus, G. Nolze. POWDER CELL – a program for the representation and manipulation of crystal structures and calculation of the resulting X-ray powder patterns. *J. Appl. Crystallogr.* **29**, 301 (1996).

23. L. Akselrud, Y. Grin. WinCSD: software package for crystallographic calculations (Version 4). *J. Appl. Crystallogr.* **47**, 803 (2014).

24. B. Andriyevsky, M. Jaskólski, V.Y. Stadnyk, M.O. Romanyuk, Z.O. Kashuba, M.M. Romanyuk. Electronic band structure and influence of uniaxial stresses on the properties of K_2SO_4 crystal: ab initio study. *Comput. Mater. Sci.* **79**, 442 (2013).

25. V.M. Gaba, V.Y. Stadnyk, O.S. Kushnir. Temperature changes of refractive indices of uniaxially compressed K_2SO_4 crystals. *Opt. Spectrosc.* **110**, 967 (2011).

26. O.V. Bovgyra, V.I. Stadnyk, O.Z. Chyzh. Energy band structure and refractive properties of $LiRbSO_4$ crystals. *Phys. Solid State* **48**, 1268 (2006).

27. V.Y. Stadnyk, M.O. Romanyuk, R.S. Brezvin. Optical and electronic parameters of $RbNH_4SO_4$ crystals. *Ferroelectrics* **192**, 203 (1997).

28. M.O. Romanyuk, A.S. Krochuk, I.P. Pashuk. *Optics* (Lviv Nat. Univ, 2012) (in Ukrainian).

29. M.O. Romanyuk. *Workshop on Crystal Optics and Crystal Physics* (Lviv Nat. Univ., 2012) (in Ukrainian).

30. O.L. Anderson. The relation between refractive index and density of minerals related to the Earth's mantle. *J. Geophys. Res.* **70**, 1463 (1965).

31. D. Adamowska. Dichte und Lichtbrechung der Moldavite von Něchov. *J. Contrib. Miner. Petrol.* **16**, 204 (1967).

32. S. Maj. On the relationship between refractive index and density for SiO_2 polymorphs. *Phys. Chem. Miner.* **10**, 133 (1984).

33. K. Sangwal, W. Kucharczyk. Relationship between density and refractive index of inorganic solids. *J. Phys. D* **20**, 522 (1987).

34. O.S. Kushnir, P.A. Shchepanskyi, V.Yo. Stadnyk, A.O. Fedorchuk. Relationships among optical and structural characteristics of $ABSO_4$ crystals. *Opt. Mater.* **95**, 109221 (2019).

35. J.L. Dhay, J.H. Wernick. *Ternary Chalcopyrite Semiconductors: Growth, Electronic Properties and Application* (Pergamon Press, 1975).

В.Й. Стадник, П.А. Щепанський,
М.Я. Рудиш, Р.Б. Матвіїв, Р.С. Брезвін

КОНЦЕНТРАЦІЙНІ ЗАЛЕЖНОСТІ
ДІЕЛЕКТРИЧНИХ ПАРАМЕТРІВ ДОМІШКОВИХ
КРИСТАЛІВ K_2SO_4

Досліджено вплив концентрації домішки міді на параметри елементарної комірки, зонно-енергетичну структуру та рефрактивні характеритики кристалів сульфату калію. Встановлено, що параметри та об'єм елементарної комірки домішкових кристалів майже лінійно зростають зі збільшенням концентрації домішки порівняно з чистим кристалом, тоді як показники заломлення n_i домішкових кристалів дещо зменшуються ($\sim 2{,}5 \cdot 10^{-3}$), однак співвідношення між ними ($n_z > n_x > n_y$ та $dn_z/d\lambda > dn_x/d\lambda > dn_y/d\lambda$) залишаються незмінними. Розраховано зонно-енергетичну структуру кристалів з 1,7% вмістом міді та виявлено, що зі зростанням концентрації ширина забороненої зони зменшується. Виявлено п'ять локалізованих рівнів у забороненій зоні, що відповідають d-електронним станам домішкових іонів Cu^{2+}. Встановлено, що вершина валентної зони утворена p-станами кисню, а дно зони провідності – $3s$- та $4s$-станами атомів сірки і калію. Біля дна зони провідності розташовані локалізовані $4s$-стани атома міді. Проаналізовано зміни параметрів елементарної комірки, показника заломлення та двопроменезаломлення, ширини забороненої зони, густини кристалів із зміною концентрації домішки міді у матриці кристала сульфату калію, а також отримано відповідні концентраційні залежності.

К л ю ч о в і с л о в а: кристал, домішка, показник заломлення, двопроменезаломлення, елементарна комірка, зонно-енергетична структура, заборонена зона.